

Heat capacity and torsional oscillator studies of molecular hydrogen in porous Vycor glass

R. H. Torii, H. J. Maris, and G. M. Seidel

Department of Physics, Brown University, Providence, Rhode Island 02912

(Received 27 December 1988; revised manuscript received 14 December 1989)

We have measured the heat capacity of para-hydrogen in a series of samples of porous Vycor glass at temperatures in the range 0.6 to 12 K. For hydrogen in the samples with large pores a freezing transition is observed; in the small-pore samples there is no feature that can be associated with a liquid-solid transition. At low temperatures the heat capacity of hydrogen in Vycor is found to decrease as the amount of hydrogen in the pores increases. We discuss possible explanations for this behavior. For hydrogen in small-pore Vycor we have made a search for superfluidity down to 0.08 K. No sharp transition is observed down to this temperature.

I. INTRODUCTION

If molecular hydrogen were a classical material it would freeze¹ at ≈ 26 K. However, because of quantum-mechanical zero-point motion, which is larger in the solid than in the liquid, the actual freezing temperature of para-hydrogen ($p\text{-H}_2$) is lowered to 13.8 K. By making an extrapolation of the free energy of the liquid (which is experimentally measured only down to the triple point T_3) to low temperatures, it has been estimated² that the difference in the energies of liquid and solid H_2 at $T=0$ K is only ≈ 6 K. This small difference is to be compared with the total binding energy in the solid which is ≈ 90 K. Thus, liquid H_2 is very close to being the stable phase even down to $T=0$ K.

In this paper we study the properties of $p\text{-H}_2$ in porous Vycor glass. An earlier experiment³ showed that in Vycor glass of pore diameter 54 Å, hydrogen froze at $T_f=9.9$ K. It is natural to assume^{3,4} that the depression of the T_f occurs because when the hydrogen is in a porous material there is a large surface term in the free energy. If α_{LW} is less than α_{SW} (α_{LW} and α_{SW} are the surface energies between liquid and solid hydrogen and the Vycor wall, respectively), the freezing temperature will be lowered. This suppression ΔT of T_f (at least for small ΔT) is proportional to r^{-1} , where r is the radius of the pores. Thus, the possibility exists that for pores of sufficiently small radius the surface contribution to the free energy is sufficiently large that the hydrogen remains liquid down to $T=0$ K. To investigate this possibility we have measured the heat capacity of $p\text{-H}_2$ in a series of Vycor glass samples with different pore sizes, as a function of the amount of H_2 in the pores. The experimental method is described in Sec. II and a brief summary of the results is given in Sec. III. In Sec. IV we give a discussion of various aspects of the data and describe the results of a search for superfluidity of H_2 at low temperatures.

II. EXPERIMENTAL METHOD

A. Porous Vycor glass

The substrates used in these experiments were porous silica glass samples produced by Corning under the trade name Vycor. Porous Vycor glass is made by the following procedure: (1) First a sodium borosilicate glass is formed, (2) heat treatment causes the glass to phase separate into a sodium-borate-rich phase and a silica-rich phase, and (3) the sodium-borate-rich phase is leached away with an acid leaving a glass with a 96 mol % SiO_2 composition and an open volume of highly interconnected cylindrical pores. For a set sodium borosilicate glass composition, the pore diameter can be altered by varying the heat treatment.⁵ We received a series of Vycor samples in the form of plates ($4 \times 1.5 \times 0.17$ cm³) which had average pore diameters from 20 to 60 Å. To prepare for either a heat capacity or a torsional oscillator experiment, a Vycor plate was roughly cut into a 1.27-cm-diam, 0.17-cm-thick disk. It had a typical mass of ≈ 0.3 g.

The Vycor surface was cleaned of organic impurities by soaking it in room-temperature hydrogen peroxide for a few days. It was then rinsed in isopropyl alcohol, acetone, and distilled water.⁶ To remove inorganic impurities, the Vycor was left soaking in room-temperature nitric acid for a few days. It was then thoroughly rinsed with distilled water. The wet Vycor was dried by placing it in a furnace and ramping its temperature to 125 °C over a 3-h period. The Vycor was then stored in either a dry nitrogen or helium atmosphere.

The substrate characteristics of the seven different Vycor samples used in these experiments are listed in Table I. The volume of pore v_{pore} per unit mass of Vycor was determined by measuring at 77 K the amount of N_2 needed to fill the pores with liquid. It was assumed that

TABLE I. Substrate characteristics for the seven Vycor samples. S_{pore} , s_{pore} , and v_{pore} are the total surface area of the sample, the surface area per unit mass, and the pore volume per unit mass, respectively. ρ and p are the density and porosity, respectively. r_{av} is the average pore radius.

Sample	I	II	III	IV	V	VI	VII
S_{pore} (m ²)	108	121	130	104	62	28.5	25
s_{pore} (m ² /g)	450	440	425	350	220	280	250
v_{pore} (cm ³ /g)	0.251	0.252	0.256	0.262	0.278	0.354	0.354
ρ (g/cm ³)	1.41	1.41	1.40	1.39	1.36	1.23	1.23
p	0.35	0.36	0.36	0.36	0.38	0.44	0.44
r_{av} (Å)	11	12	12	15	25	25	29

the pores were filled with liquid when the N₂ pressure was raised to 0.95 of the saturated vapor pressure. For samples I–V, the surface area s_{pore} per unit mass determined by Corning from N₂ adsorption isotherm measurements is listed in Table I. We have made similar measurements for samples I, V, VI, and VII, and our results⁷ for VI and VII are listed in the table. For the two samples I and V, on which both Corning and we made measurements, the results were in reasonable agreement.

The sample porosity p and the density ρ were determined from v_{pore} by assuming that the Vycor was composed entirely of SiO₂ with a density ρ_0 of 2.18 g cm⁻³. We have

$$p = \frac{\rho_0 v_{\text{pore}}}{(1 + \rho_0 v_{\text{pore}})}, \quad (1)$$

$$\rho = \frac{\rho_0}{(1 + \rho_0 v_{\text{pore}})}. \quad (2)$$

For a set of nonintersecting cylindrical pores of volume V and surface area S , the pore radius is $2V/S$. We therefore define an average pore radius r_{av} for our samples by

$$r_{\text{av}} = \frac{2v_{\text{pore}}}{s_{\text{pore}}}. \quad (3)$$

p , ρ , and r_{av} are listed in Table I.

The isotherms of I and V are shown in Fig. 1 as plots of the amount of N₂ adsorbed versus reduced pressure (reduced pressure is the pressure divided by the saturated vapor pressure of liquid N₂ at 77 K). For samples V–VII, the isotherms showed a definite hysteric behavior through the region of capillary condensation. According to Cole and Saam,⁸ this can be understood in the following way. Along the adsorption path the liquid film will thicken. Above a certain pressure P_m the liquid film becomes metastable, since a lower free-energy state exists (partially filled pores) which is hydrodynamically inaccessible. Cole and Saam have shown that at a critical pressure P_c (greater than P_m), a hydrodynamic instability in the film will lead to a transition to a state of partially filled pores. This reduces the film's surface area. Along the desorption path, capillary evaporation will occur at P_m . Cole and Saam's theory explains the hysteresis, and also implies that the desorption isotherm is the equilibrium process. As can be seen in Fig. 1, capillary condensation and the accompanying hysteresis are not observed for sample I.

For samples I and V–VII, we determined pore-size distributions from the desorption isotherms using the method described by Pierce⁹ as modified by Orr and Dalla Valle.¹⁰ For samples I–V, distributions were determined by Corning, also from desorption isotherms. As discussed by Gregg and Sing,¹¹ this method cannot give reliable information about pore-size distributions for radii less than a value r_{min} , which is 10 or 15 Å. The results for the pore-size distribution can be summarized as follows: (1) For the small pore samples (I–IV), the volume associated with pores of a given range of radii r decreases rapidly and monotonically with increasing r , within the range where measurements can be made ($r > r_{\text{min}}$). This is not surprising since, from Table I, one can see that the average pore radius in these samples is about equal to r_{min} . Thus we do not know if there is a peak in the distribution of pores, or if there is simply a monotonically de-

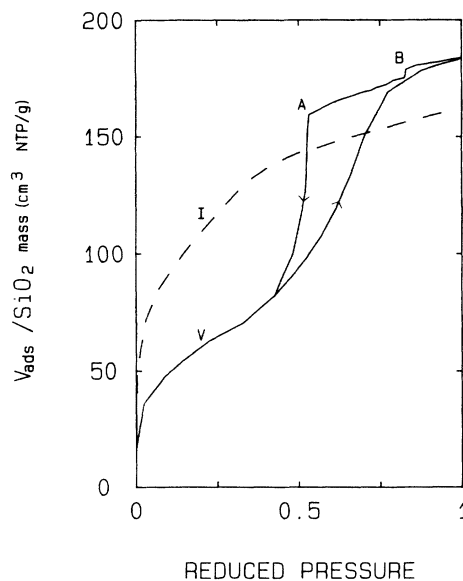


FIG. 1. N₂ adsorption isotherms for samples I and V at 77 K. The volume of N₂ gas adsorbed per unit mass of the Vycor is plotted as a function of reduced pressure (N₂ gas pressure divided by the saturated vapor pressure of liquid N₂ at 77 K). The sharp drops at A and B in the desorption isotherm for sample V are due to the emptying of pores of approximate radii 25 and 60 Å, respectively.

creasing distribution in pore radii starting at zero. (2) For the larger pore samples (V–VII), there is a peak in the pore distribution which is roughly at r_{av} , and a large fraction (at least 0.5) of the total pore volume is associated with pores in the vicinity of this peak. The peak in the distribution of radii has a half-width which is roughly 20% of the average radius. In addition, there is a secondary peak in the distribution at a radius of $\approx 60 \text{ \AA}$ (this peak is also present for sample IV). The total volume of the pores in this peak relative to the pore volume in the main peak in the distribution varied for the different samples.

B. Calorimetry

A schematic of the experimental setup used in the specific-heat measurements is shown in Fig. 2. The Vycor disk was glued with GE7031 varnish to the inside bottom of a cylindrical OFHC copper cell of mass 2.2 g. The Vycor fitted closely into the copper cell so that only a volume of $\approx 0.2 \text{ cm}^3$ was not occupied by the Vycor. Once the varnish had dried, the cell with the top off was placed in a dessicator in order to pump on the Vycor for several hours. The cell was then removed from the dessicator and the cell top was sealed to the body with low-

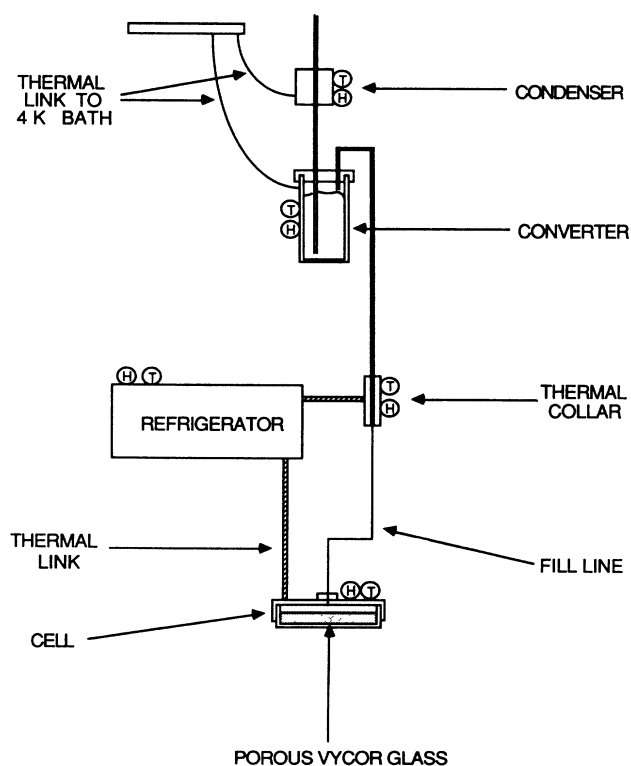


FIG. 2. Schematic diagram of the low-temperature heat capacity apparatus. The refrigerator was either a ^4He pot (1.5 K) or ^3He pot (0.5 K). H and T indicate heaters and thermometers, respectively.

melting-point solder while the Vycor was maintained in an atmosphere of helium gas. The cell was connected through a thermal link to a refrigerator which could be kept at a constant temperature T_0 . The refrigerator was either a continuously filled ^4He evaporator or a recirculating ^3He evaporator. The thermal link was made of either copper wire or brass shim depending upon the temperature range of measurement. The dimensions of the link were chosen to give the empty calorimeter (cell plus Vycor without H_2) a thermal-relaxation-time constant of $\approx 600 \text{ sec}$. A heater and a thermometer were also attached to the outside of the cell. The thermometer was calibrated using the vapor pressure of liquid H_2 and ^4He as well as a commercially calibrated germanium resistor.

The H_2 fill line consisted of a thermally isolated stainless-steel capillary [0.025-cm inside diameter (i.d.)], which ran from a valve at room temperature down the cryostat to a copper bushing (condenser) whose temperature could be controlled in the range up to 20 K. The capillary continued past the condenser by 5 cm and then entered a copper can (converter) filled with neodymium oxide (Nd_2O_3) powder. The Nd_2O_3 powder catalyzes the conversion of H_2 molecules between the ortho and para state. The temperature of the converter could also be controlled. To avoid possible time varying heat leaks to the calorimeter via the H_2 fill line, the midpoint of the CuNi capillary (0.015-cm i.d., 20-cm long) connecting the converter to the calorimeter was attached to a thermal collar, the temperature of which was controlled electronically to follow the temperature of the calorimeter.

The calorimeter was mechanically supported by its thermal link and by nylon line connected to the refrigerator. The low-temperature part of the apparatus hung in a stainless-steel can under high vacuum. Exchange gas was not used in the vacuum can prior to cooling to 4 K since any residual helium gas which could not be pumped out interfered with the heat capacity measurements. The cool down from 77 to 4 K typically took 5 h.

A specific amount of H_2 gas was transferred to the Vycor using standard gas-handling techniques. From a high-pressure cylinder, 99.99% pure H_2 gas was passed through a molecular sieve cold trap at 77 K into an accurately known volume of 150 cm^3 . The amount of H_2 removed from this volume and admitted to the apparatus could be determined with an accuracy of 1%. To ensure that the H_2 adsorbs into the Vycor, the following procedure was adopted. The condenser was initially at a temperature of 15 K and the calorimeter was set at a temperature of 14–20 K depending upon the amount of H_2 already adsorbed in the Vycor. The converter temperature was chosen so that the H_2 gas would adsorb onto the Nd_2O_3 powder before entering the Vycor. Once the Nd_2O_3 powder was full of H_2 , both the condenser and the converter were heated to 20 K so that by surface adsorption or capillary action the H_2 would transfer into the Vycor. The H_2 equilibrium ortho-para ratio at 20 K is 0.002.

The heat capacity was measured by using a thermal-relaxation method.¹² This technique required two independent measurements to find the heat capacity at each

temperature. These were (1) the heat flow, dQ/dt , across the thermal link between the calorimeter and the refrigerator as a function of calorimeter temperature, and (2) the calorimeter cooling rate dT/dt in the absence of a heat input. The heat capacity was then given by $-(dQ/dt)/(dT/dt)$. The conductance of the thermal link was measured as a function of calorimeter temperature by applying a voltage to the calorimeter heater and then recording the steady-state calorimeter temperature, while maintaining the refrigerator temperature at T_0 . To measure the calorimeter cooling rate, the calorimeter was heated from T_0 to some high temperature and then with no heat input allowed to cool back to T_0 . The cooling rate was determined from the slope of the cooling curve.

The calorimeter temperature was recorded as a function of time using a computer. The computer and associated electronics were also used to determine the temperature of thermometers attached to the refrigerator and to the thermal cooler. These temperatures were controlled in a standard manner by the computer using joule heating. The computer control also made possible warming runs in which the heat input to the calorimeter was continuously adjusted and was larger than the heat flow through the thermal link.

This thermal-relaxation method has the advantage that the heat capacity is measured continuously with temperature. In addition, when the sample undergoes a phase transition, the rate of cooling decreases and is identifiable on the cooling curve. In Fig. 3, a sample data set is shown displaying these features. The heat capacity of the empty calorimeter (i.e., including the Vycor but without H_2) was measured first and then subtracted from the measurements with H_2 coverages. The resultant heat capacity for H_2 had an error which was estimated to be no greater than $\pm 5\%$.

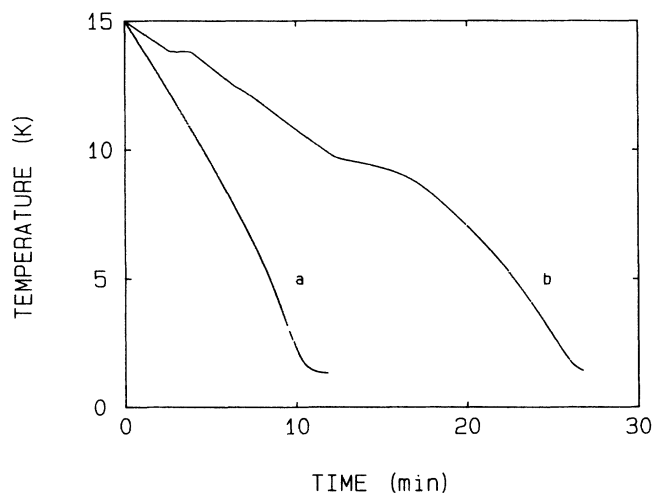


FIG. 3. Representative cooling curves from which the heat capacity can be determined. Curve *a* shows the empty calorimeter and *b* the calorimeter with H_2 . In *b* the feature at 14 K is due to H_2 freezing outside of the Vycor pores and the feature at 10 K is due to freezing of H_2 in the pores.

C. Torsional oscillator

The torsional oscillator used in these experiments was of a design similar to that developed and used at Cornell.¹³ The large mass, torsion rod, and cell were machined from a single cylindrical piece of BeCu. A hole was drilled axially through the large mass and torsion rod to serve as a fill line to the cell, the CuNi capillary being soldered to the BeCu at the large mass. The Vycor sample was attached to the cell with GE7031 varnish. Before the cell was sealed with a BeCu cap, the oscillator was placed in a dessicator so that the Vycor could be pumped on for several hours. The oscillator with the Vycor had a resonant frequency of about 2000 Hz and a Q at a low temperature of 5×10^5 . The frequency of the oscillator could be measured to 5 parts in 10^8 at low temperatures.

A heater and thermometer were attached to the large mass with GE7031 varnish. For the temperature range 6 to 0.6 K, the heater, thermometer, and H_2 fill line were the same as those used in the heat capacity experiment. For measurements made down to 0.08 K, the refrigerator was the mixing chamber of a dilution refrigerator. The oscillator was suspended from the appropriate refrigerator by four stainless-steel springs attached to the top of the large mass.

The cell was driven and its motion was detected electrostatically. A drive electrode and a detector electrode were epoxied into a BeCu structure which was attached with screws and vacuum grease to the large mass. Both electrodes were dc biased to 250 V. An ac voltage was applied to the drive electrode and the ac response of the detector electrode was measured by a lock-in amplifier. The oscillator resonant frequency was found by adjusting the drive frequency until the real part of the detector signal was zero. The ac voltage for the drive was produced by a voltage controllable 20-MHz synthesizer. It was stepped down in frequency by a factor of 10^4 and then amplified by the reference channel of the lock-in. The synthesizer and the counter used to measure the frequency were referenced to a rubidium vapor frequency standard stable to 1 part in 10^{10} /month. A computer was used to measure and control the temperature of the oscillator as well as to measure its frequency and adjust the drive frequency of the synthesizer. Data points were taken at a rate of 3 h^{-1} .

III. HEAT CAPACITY RESULTS

A. Heat capacity for full Vycor

In this section we present a brief summary of the principal features of the results. The heat capacity of Vycor samples I–VII with the pores full of $p\text{-}H_2$ was measured from 2 to 16 K and the results (plotted as specific heat) are shown in Fig. 4. We were able to determine that sufficient H_2 had been added to fill the pores in the following way. Due to capillary action, it is energetically favorable at 14 K for liquid H_2 to be in the Vycor pores rather than outside of the pores. Thus, the presence of a bulk H_2 freezing transition at 13.8 K implies that the pores are full (one can see this transition in each curve in

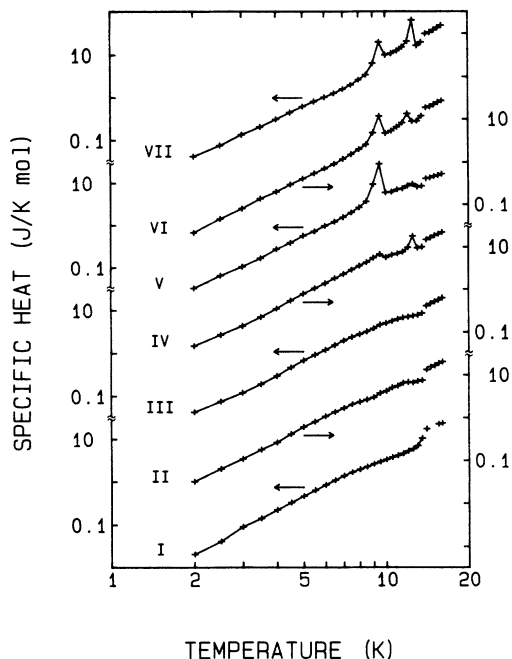


FIG. 4. Specific heat of p -H₂ in the Vycor samples I–VII as a function of temperature. Curves are displaced vertically to separate them.

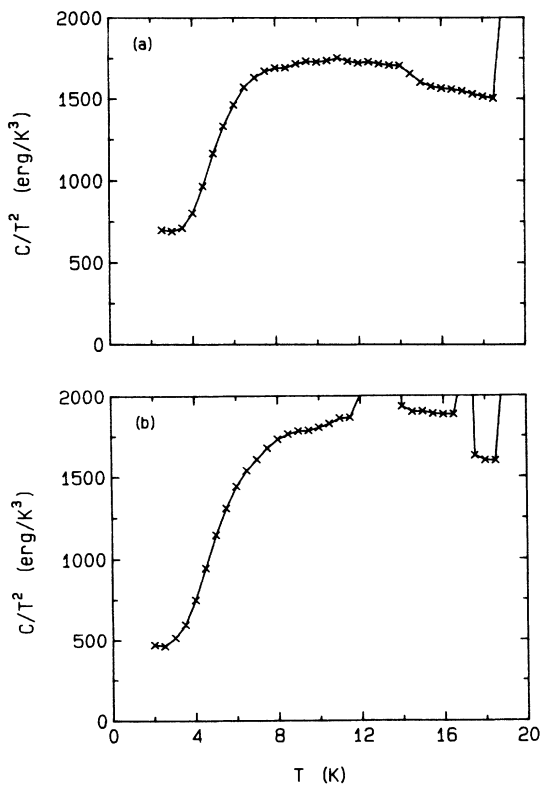


FIG. 5. Heat capacity C of o -D₂ in samples III and IV plotted as C/T^2 vs T . (a) Sample III. (b) Sample IV.

Fig. 4). The small amount of bulk H₂ outside of the Vycor makes a negligible contribution to the measured heat capacities below 13.8 K. One can see in Fig. 4 that, except at temperatures close to freezing transitions, the specific-heat measurements for all seven samples have similar temperature dependences and magnitudes. At low temperatures, the specific heat of H₂ in all seven samples had approximately a T^3 temperature dependence.

For small-pore samples I–III shown in Fig. 4, we did not observe freezing of H₂ in the Vycor pores. For samples IV–VII, we observed two different freezing transitions for H₂ in the Vycor pores. For each sample, the two freezing transitions (T_{f1} and T_{f2}) below 13.8 K are believed to be due to the two distinct pore radii in the pore-size distribution as discussed in Sec. II A. For sample IV, the freezing transitions in the Vycor pores are observed at temperatures $T_{f1}=9.3$ K and $T_{f2}=12.4$ K. For samples V–VII, T_{f1} shifted to 9.5 K and T_{f2} remained at 12.4 K.

For samples III and IV, the heat capacity of the Vycor pores full of o -D₂ was measured from 2 to 20 K as shown in Fig. 5 as C/T^2 versus T . Sample III did not show a D₂ freezing transition in the pores whereas sample IV did exhibit freezing transitions at 13 and 17.5 K. The bulk triple point of o -D₂ is 18.7 K. At low temperatures below 3 K, C/T^2 rises in both samples. We believe this is due to the partial ordering of a small amount ($< 2\%$) of p -D₂. The deuterium was converted by a catalyst at 20 K [which should give a p -D₂ concentration of 2% (Ref. 14)], and further conversion occurred while D₂ was in the Vycor before the specific-heat measurement was taken. Thus, the p -D₂ concentration may be different in the two samples.

B. Heat capacity of partially filled Vycor

Measurements as a function of filling were made for samples I, III, V, and VII. The numbers of different coverages studied in the range 2 to 16 K were 12, 8, 7, and 6 for these four samples, respectively. For sample III, the temperature range was extended down to 0.7 K for four coverages (including full pores). Results for C/T^2 for samples I and V are shown in Figs. 6 and 7, and the low-temperature data for sample III are in Fig. 8.

We can summarize the results for the freezing of H₂ as a function of coverage as follows. No freezing transition was observed at any coverage for samples I–III. For IV–VII, no freezing was observed until a critical filling was reached. Samples V and VII were studied in detail. For V, above this critical filling the temperature T_{f1} of the lower freezing transition and the latent heat at this transition increased monotonically as extra H₂ was added. The lowest T_{f1} for sample V was 8.5 K at a fractional filling f of 0.63 (fractional filling is defined as the amount of H₂ in the Vycor pores divided by the amount of H₂ which completely fills the pores). The transition at T_{f2} was observed only when the pores were full of H₂, i.e., for the first filling at which a bulk freezing transition was observed. Presumably, there is a small range of fractional fillings below 1 where T_{f2} can still be observed, but we

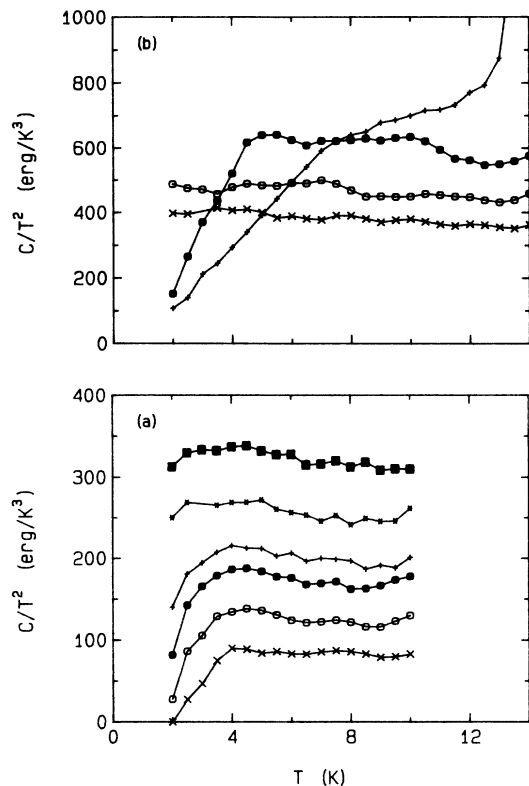


FIG. 6. Heat capacity C for sample I as a function of p -H₂ filling plotted as C/T^2 vs T . (a) Low-coverage data in mmol: (\times) 0.35, (\circ) 0.51, (\bullet) 0.65, ($+$) 0.79, ($*$) 0.93, (\blacksquare) 1.07. (b) Higher-coverage data in mmol: (\times) 1.24, (\circ) 1.40, (\bullet) 1.80, ($+$) 2.10.

have not checked this point. For sample VII, the lower freezing transition at $T_{f1}=9.5$ K first appeared for $f=0.71$. When f was increased T_{f1} decreased slightly and reached a minimum value of 9.3 K for f of 0.98. The

TABLE II. Results for the low-temperature heat capacity. b is the coefficient of the T^2 term in the heat capacity. T_1 is the temperature below which the heat capacity begins to decrease very rapidly.

Sample	Amount (mmol)	Coverage ($\mu\text{mol m}^{-2}$)	b (K^{-3})	T_1 (K)
I	0.35	3.2	0.0029	4.0
I	0.51	4.7	0.0030	3.6
I	0.65	6.0	0.0031	3.2
I	0.79	7.3	0.0031	2.4
I	0.93	8.6	0.0033	2.0
I	1.07	9.9	0.0036	1.8
I	1.24	11.5	0.0037	
I	1.40	13.0	0.0041	
III	0.50	3.8	0.0048	3.7
III	0.75	5.8	0.0048	2.8
III	1.00	7.7	0.0048	2.0
III	1.25	9.6	0.0048	
III	1.50	11.5	0.0048	
V	0.50	8.1	0.0042	2.2

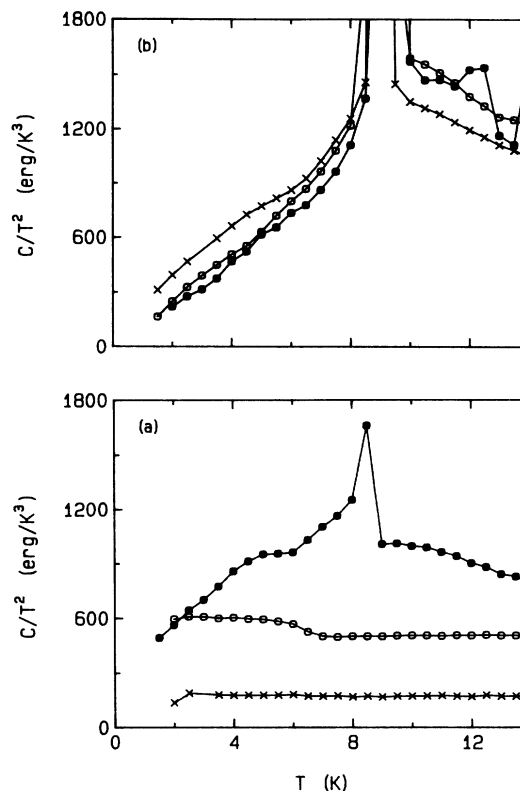


FIG. 7. Heat capacity C for sample V as a function of p -H₂ filling plotted as C/T^2 vs T . (a) Low-coverage data in mmol: (\times) 0.50, (\circ) 1.00, (\bullet) 1.50. (b) Higher-coverage data: (\times) 1.90, (\circ) 2.20, (\bullet) 2.70.

latent heat also decreased slightly throughout this range of f . For $f=1$, T_{f1} moved to 9.6 K, and the latent heat increased. The transition at T_{f2} was observed to have a temperature and latent heat which increased monotonically.

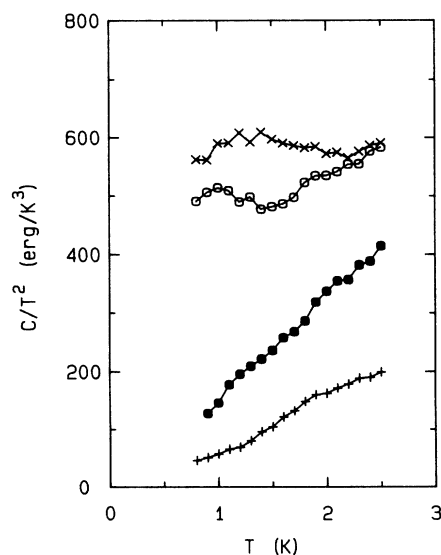


FIG. 8. Low-temperature heat capacity C of sample III as a function of p -H₂ filling plotted as C/T^2 vs T . H₂ coverage in mmol: (\times) 1.50, (\circ) 1.75, (\bullet) 2.00, ($+$) 2.25.

cally from $f=0.85$ to 1. The lowest T_{f2} for sample VII was equal to 11.5 K at a fractional filling of 0.85.

We now describe general features of the specific-heat results which are dependent on the fractional filling and which have a qualitatively similar form in both the small-pore samples (I and III) and the large-pore samples (V and VII). For small fillings the heat capacity had a T^2 dependence down to a temperature T_1 (Table II). Below T_1 , C decreased much more rapidly with decreasing T . The temperature T_1 was observed to decrease as the amount of H_2 increased. This behavior can be seen in the small filling curves of Figs. 6 and 7.

The decrease in T_1 with increasing coverage continued until a coverage was reached which displayed no sharp drop in heat capacity, i.e., the heat capacity varied as T^2 down to the lowest temperature of measurements. When the H_2 filling was increased beyond this point, the heat capacity at low temperatures decreased as the amount of H_2 increased. Thus, in this regime the specific heat is decreasing very rapidly with increasing filling (see Table II).

IV. DISCUSSION

In this section we compare the data with the heat capacity expected on the basis of several simple models.

A. Phase diagram

It is convenient to summarize the results in partially filled Vycor by means of a "phase diagram." This is shown in Fig. 9 and has been obtained by combining data

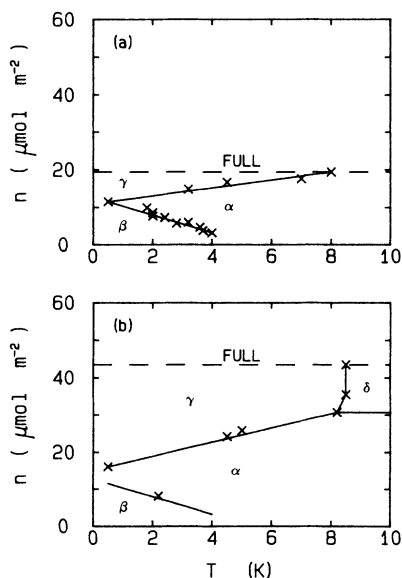


FIG. 9. "Phase diagram" in the coverage (n)-temperature plane for partially filled Vycor. (a) and (b) for small-pore (samples I and III) and large-pore (samples V and VII) Vycor, respectively. The behavior of the heat capacity in the different phases is discussed in the text. The dashed line corresponds to full Vycor (for samples I and V). The solid lines through the data points are intended as a guide to the eye.

from I and III (small pore) to form Fig. 9(a) and data from V and VII (large pore) to form Fig. 9(b). Of course, the "phases" we refer to are not necessarily separated by sharp transitions, they may simply be regions of coverage-temperature (n - T) plane in which the heat capacity varies with n and T in a particular way. Below 8 K both small- and large-pore Vycor have three phases, and the boundaries between these phases lie in approximately the same places in the n - T plane. The properties of these phases are as follows: (α) The heat capacity C is proportional to T^2 . For submonolayer coverages C is also roughly proportional to the amount of H_2 present. Thus, the specific heat c is approximately independent of coverage. (β) The heat capacity decreases very rapidly with decreasing T and quickly becomes too small to measure at low temperatures. (γ) C is proportional to T^3 and decreases with increasing coverage. Thus, c is decreasing very rapidly as H_2 is added.

The phase diagram is bounded for large coverages by the line in the n - T plane where the Vycor is just full (dashed line in Fig. 9). We have taken this as the coverage at which bulk latent heat of freezing first occurs,¹⁵ and have assumed that the amount of H_2 needed to fill the Vycor is independent of temperature.

For small-pore Vycor it appears that the α - γ line intersects the line corresponding to just-full Vycor at between 8 and 9 K. There is thus no evidence for phases other than α , β , and γ in small-pore Vycor. In large-pore Vycor the situation at high temperature is more complex. When the filling is sufficiently large one observes the transitions T_{f1} and T_{f2} , which we have assumed are freezing transitions of H_2 in small and large pores, respectively. We therefore include a region δ in the phase diagram [see Fig. 9(b)]. In δ the heat capacity is an increasing function of filling and varies with temperature approximately as T , i.e., more slowly than in α . We do not have data close to the α - δ boundary, and so the location of the line in Fig. 9(b) is just a guess.

B. Comparison to results for ^4He in Vycor

The specific heat of ^4He in one sample of Vycor glass (similar to our large-pore samples) has been studied by Tait and Reppy,¹⁶ and recently more detailed measurements with higher accuracy have been reported by Chan and co-workers.^{17,18} Reppy and Tait proposed the phase diagram which is shown in Fig. 10. This phase diagram is very similar in form to the diagram we have obtained. In addition, the heat capacities in the different phases have some similarity to what we have observed. In phase A, C increases with coverage and varies as $(aT + bT^2)$. Crossing into the B phase the heat capacity drops rapidly, just as it does going from the α to the β phase for H_2 . In the C phase the heat capacity drops rapidly with increasing filling, just as in our γ phase.

This correspondence between the phase diagrams is remarkable when one considers the properties of the individual phases for ^4He . Tait and Reppy show that the α - γ line coincides with the transition to superfluidity as determined by torsional oscillator measurements. Thus, if we accept the correspondence of the phase diagrams, the γ

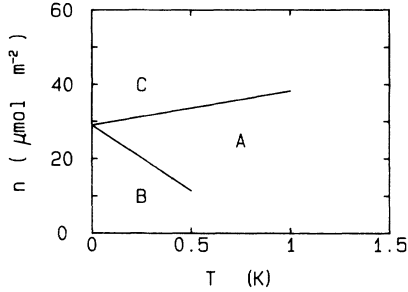


FIG. 10. Phase diagram for ${}^4\text{He}$ on porous Vycor glass proposed by Tait and Reppy (Ref. 16).

region of our phase diagram would correspond to superfluid H_2 . Is this a serious possibility? We had earlier estimated² that liquid H_2 might become superfluid at 2 or 3 K, whereas the γ phase exists up to 8 K. On the other hand, it had earlier been predicted by Ginzburg and Sobyenin¹⁹ that T_λ for H_2 should be close to the ideal Bose gas value (6 K), and might be even larger. Thus, the temperature range of the γ phase may not rule out superfluidity. However, the peak in the heat capacity that occurs between the γ and δ phases has characteristics that strongly suggest that freezing occurs on the γ - δ line, and hence the phase γ is solid. (This assumption was already made in Sec. III.) As will be shown later, the area under the peak is roughly what is expected given the known latent heat of fusion of H_2 . In addition, the temperature at which the peak occurs is higher if the specific heat is measured while the temperature is increased.²⁰ Hysteresis is characteristic of a first-order phase transition and would not normally be expected to occur at a simple λ transition. Given that the γ phase in large-pore Vycor is solid, does this mean that γ in small-pore Vycor is also solid? The heat capacity of the γ phase in large- and small-pore Vycor is very similar (see Figs. 6 and 7) and this implies that in small-pore Vycor the γ phase is also solid.

Tait and Reppy¹⁶ proposed that the B phase consisted of monolayer islands, and that A was the same structure but in a temperature range where some two-dimensional (2D) evaporation could occur. In the next sections we will consider whether this type of model can explain our data in the α and β phases.

C. H_2 -Vycor interaction

To determine the interaction between H_2 and the Vycor substrate we measured the adsorption isotherm of H_2 in sample I. This gave an isosteric heat of adsorption at 15 K of 580 K, which implies that the binding energy U_0 at $T=0$ K is 540 K (± 50 K). We model the interaction between a H_2 molecule and a substrate atom by a Lennard-Jones potential of depth ϵ_v and distance to the minimum a . If the substrate (Vycor) atoms are taken to be uniformly distributed in the region $z < 0$, the potential for $z > 0$ is given by

$$U(z) = \frac{\pi n_v a^3 \epsilon_v}{3} \left[\frac{1}{15} \left(\frac{a}{z} \right)^9 - \left(\frac{a}{z} \right)^3 \right], \quad (4)$$

where n_v is the number density of the atoms in Vycor. The depth of the potential minimum is

$$U_{\min} = 1.5611 \epsilon_v n_v a^3 \quad (5)$$

at the distance z_{\min} of $0.7647a$. At the minimum the spring constant for motion normal to the surface is

$$\frac{d^2 U}{dz^2} = 46.17 \frac{U_{\min}}{a^2}. \quad (6)$$

Hence, in the harmonic approximation the vibrational frequency is

$$\omega = (46.17 U_{\min} / m a^2)^{1/2}. \quad (7)$$

If we now choose U_{\min} so that

$$-U_{\min} + \frac{1}{2} \hbar \omega = -U_0, \quad (8)$$

we obtain [setting a equal to the same distance (3.32 \AA) as in the H_2 - H_2 interaction²¹]

$$U_{\min} = 670 \text{ K}, \quad (9)$$

$$\hbar \omega = 260 \text{ K}. \quad (10)$$

Thus, at the temperatures of interest here, the motion of the H_2 normal to the surface is frozen out.

Consider now the variation of the potential parallel to the substrate. For helium Tait and Reppy¹⁶ have explained their data by proposing that there is a long-range variation of the substrate potential as a function of position on the surface. Such a variation could come about from the curvature of the wall of the Vycor pore. If the principle radii of curvature of the wall are R_1 and R_2 , it is straightforward to show that to lowest order in curvature the change in potential at distance z from the wall is

$$\delta U(z) = \frac{\pi n_v a^4 \epsilon_v}{4} \left(\frac{1}{R_1} + \frac{1}{R_2} \right) \left[\frac{1}{20} \left(\frac{a}{z} \right)^8 - \left(\frac{a}{z} \right)^2 \right]. \quad (11)$$

Thus,

$$\frac{\delta U_{\min}}{U_{\min}} = 0.645a \left(\frac{1}{R_1} + \frac{1}{R_2} \right). \quad (12)$$

Hence, for example, the potential at the surface of a spherical pore in large-pore Vycor (diameter $\approx 50 \text{ \AA}$) will be greater than the potential at a flat surface by 115 K. In small-pore Vycor the variation will be roughly twice as large.

In addition to this long-range variation of the potential, there will also be short-range variations. These must be of the same order of magnitude as the strength of the interaction with individual substrate atoms. The number density of atoms (Si and O) in fused silica is $6 \times 10^{22} \text{ cm}^{-3}$. If we use this value for n_v in Eq. (5) we obtain

$$\epsilon_v \approx 200 \text{ K}. \quad (13)$$

To decide whether 2D islands should form, we have to compare the variation in the substrate potential with the binding Φ_I of a H_2 molecule to other molecules in a 2D island. This binding has been calculated by Ni and Bruch,²² and their result is

$$\Phi_I = 22 \text{ K} . \quad (14)$$

Let us imagine that we begin to add H_2 to empty Vycor. Initially, an island will form in the surface region where the substrate potential is strongest.²³ As this island grows the extra H_2 molecules are added around the edge of the island, where the substrate potential is weaker. When the substrate potential at the edge added to Φ_I becomes less than the strength of the substrate potential at some other point on the surface, the island will stop growing and a new island will begin to develop. Since Φ_I appears to be considerably smaller than the expected variation in the substrate potential, we expect that for a submonolayer coverage the H_2 will be in the form of 2D islands. The size of the islands should be comparable to the pore radius.

D. Heat capacity for submonolayer coverage

1. Contribution from 2D phonons

To estimate the specific heat of a submonolayer layer of H_2 we first consider a simplified model. We assume for the moment that the islands are completely free to slide relative to the substrate. In addition, we consider the islands to be large compared to the wavelength of thermal phonons, i.e.,

$$D_I \gg \frac{h\nu}{kT} , \quad (15)$$

where ν is the speed of sound in the island, and D_I is the diameter of the island. The 2D density of phonon states per unit area is then approximately

$$g(\omega) = \frac{\omega}{\pi v^2} \quad (16)$$

with

$$\frac{1}{v^2} = \frac{1}{2} \left[\frac{1}{v_l^2} + \frac{1}{v_t^2} \right] , \quad (17)$$

where v_l and v_t are the velocities of longitudinal and transverse waves in the island. Then,

$$C = \frac{2.296}{v^2} \nu R a_m \left[\frac{kT}{\hbar} \right]^2 , \quad (18)$$

where a_m is the area occupied by one molecule. a_m for 2D solid H_2 has been calculated by Ni and Bruch.²² For an uncompressed H_2 monolayer they find

$$a_m = 14.3 \text{ \AA}^2 . \quad (19)$$

They have also calculated the enthalpy as a function of lattice constant, and from this the two-dimensional "bulk" modulus B_2 ($B_2 = -A\delta P/\delta A$ with P the surface

pressure and A the area) can be found. It is straightforward to show that the longitudinal and transverse sound velocities v_l and v_t in the monolayer are

$$v_l = \left[\frac{2B_2}{\rho_2(1+\sigma)} \right]^{1/2} , \quad (20)$$

$$v_t = \left[\frac{B_2(1-\sigma)}{\rho_2(1+\sigma)} \right]^{1/2} , \quad (21)$$

where σ is the 2D Poisson's ratio. Thus,

$$v^2 = \frac{4B_2(1-\sigma)}{\rho_2(1+\sigma)(3-\sigma)} . \quad (22)$$

For the uncompressed monolayer²⁴ B_2 has the value $\approx 30 \text{ g sec}^{-1}$ and so, assuming²⁵ the value $\frac{1}{4}$ for σ , we obtain

$$v = 1.1 \times 10^5 \quad (23)$$

in cm sec^{-1} . From Eq. (18) we obtain

$$C = 0.0050 T^2 \nu R \quad (24)$$

in K^{-1} . (If we had chosen σ as $\frac{1}{3}$, for example, we would have a heat capacity 16% larger.)

To make a comparison of this result to the experimental data, we have fitted the data in the appropriate temperature range to the form $bT^2\nu R$ to determine the coefficient b . The results lie in the range 0.0029 to 0.0048 K^{-3} (see Table II), to be compared with the theoretical value $b_{\text{th}} = 0.005 \text{ K}^{-3}$. Thus, the experimental heat capacity is generally in reasonable agreement with the theory, but for most of the data sets it is somewhat smaller.

Despite this near agreement there are serious problems with this model. The lateral variations of the substrate potential will compress the islands and raise the sound velocity. Within an island the chemical potential must be constant. The chemical potential is the sum of the binding energy to the substrate, which we take to be U_{min} , and μ_{2D} , the chemical potential for a H_2 molecule in a 2D film at local density. For μ_{2D} we use the calculations of Ni and Bruch,²² which are for strictly 2D H_2 . Then,

$$U_{\text{min}} + \mu_{2D} = \text{const} . \quad (25)$$

For a 2D island in the absence of any lateral potential μ_{2D} has the value²² -22 K . This will be the value μ_{edge} of μ_{2D} at the edge of the island. Hence, the chemical potential $\mu_{2D}(\mathbf{r})$ at some interior point \mathbf{r} will be

$$\begin{aligned} \mu_{2D}(\mathbf{r}) &= U_{\text{min}}^{\text{edge}} - U(\mathbf{r}) + \mu_{\text{edge}} \\ &\equiv \Delta U(\mathbf{r}) + \mu_{\text{edge}} . \end{aligned} \quad (26)$$

In large-pore Vycor we estimated from Eq. (12) that potential variations of at least 100 K can occur. If we set $\Delta U = 100 \text{ K}$ we get $\mu_{2D}(\mathbf{r}) = 78 \text{ K}$. From the calculations of Ni and Bruch²² for this value of the chemical potential the density of the 2D layer is increased by a factor of 1.19, and the bulk modulus has increased by roughly a factor of 4. Thus, the heat capacity of the whole island should be reduced substantially from the previous estimate. (Note that C is inversely proportional to both the

density and the bulk modulus.) This reduction should be even larger for small-pore Vycor (sample I).

Consider now the effect of the finite size of the islands on the phonon heat capacity. An island on a homogeneous substrate would have three phonon modes of zero frequency, and hence the heat capacity should contain a term

$$C_0 = \frac{3}{2} N_I kT, \quad (27)$$

where N_I is the number of islands. In Vycor the heterogeneity of the substrate will cause all of these modes to have a finite frequency. The variations of the substrate potential provide one restoring force. In addition, an island when it is in its location of minimum potential energy has to have a definite curvature (which varies from place to place on the island) in order to conform to the Vycor surface. If the island translates or rotates, the curvature of the island will, in general, have to change and the elastic energy of the island will also change thereby giving an extra restoring force. The restoring force due to the substrate potential can be estimated as follows. For simplicity, consider an island whose radius²⁵ R_I is comparable to the radius of curvature of the Vycor pore. The effective spring constant of the island is of the order of the number of molecules times $\delta U_{\text{min}}/R_I^2$. Hence, the order of magnitude of the frequency ω of translational vibration of the island is given by

$$\omega^2 \approx \frac{\Delta U}{mR_I^2}, \quad (28)$$

where ΔU is the magnitude of the variation in the substrate potential, and m is the mass of the H_2 molecule. If we take $\Delta U = 100$ K and $R_I = 20$ Å (plausible values for large-pore Vycor),

$$\begin{aligned} \omega &\approx 3.2 \times 10^{11} \\ &\approx 2.5 \end{aligned} \quad (29)$$

in sec^{-1} and K, respectively. The order of magnitude for the frequency of rotational vibration should be roughly the same. In a similar spirit one can estimate the restoring force due to the curvature of the island and the substrate. This makes a contribution to ω^2 which is

$$\omega^2 \approx \frac{B_2}{\rho_2 R_I^2}, \quad (30)$$

which has about the same magnitude as Eq. (28). As a result of these effects the phonon spectrum of the islands will have no modes below a frequency ω_c of $\approx 3 \times 10^{11} \text{ sec}^{-1}$. At first sight it appears that this cutoff might give a natural explanation of the drop in heat capacity that occurs on going from the α to the β phase. If the phonon density of states is

$$g(\omega) = \begin{cases} \frac{\omega}{\pi v^2}, & \omega \geq \omega_c \\ 0, & \omega < \omega_c, \end{cases} \quad (31)$$

the heat capacity is

$$C = \frac{\nu R a_m}{\pi v^2} \left(\frac{kT}{\hbar} \right)^2 \int_y^\infty \frac{x^3 e^x}{(e^x - 1)^2} dx \quad (32)$$

with $y \equiv \hbar \omega_c / kT$. In Fig. 11 we show a fit of this function to the data obtained on sample I with 0.51 mmol of H_2 . The fit uses $\nu = 0.85 \times 10^5 \text{ cm sec}^{-1}$, and $\omega_c = 1.2 \times 10^{12} \text{ sec}^{-1}$. The theoretical specific heat varies much more slowly than the data. Moreover, in a more realistic model it would clearly be necessary to allow for a distribution of values of ω_c , and this would make the disagreement with experiment even worse. It appears that this model can only explain the dropoff in C in the β phase if the cutoff frequency ω_c increases as the temperature is lowered. A temperature dependence of this type occurs at the incommensurate-commensurate transition for a monolayer on a crystalline substrate. We do not know of any theory of the analogous effect for a disordered substrate.

2. Contribution from 2D evaporation

At finite temperatures there will be a certain number N_G of H_2 molecules excited out of the islands. Because the substrate potential is much larger than kT , we only need consider molecules which leave the islands but are still adsorbed on the Vycor surface. If we consider these atoms to move freely in 2D over the surface, it is straightforward to show that the number of evaporated atoms N_G is

$$N_G = N \frac{1-f}{f} \left[\frac{2\pi\hbar^2}{mkT a_m} e^{\Delta/kT} - 1 \right]^{-1}, \quad (33)$$

where N is the total number of molecules, Δ is the energy to evaporate a molecule from an island, and f is the fraction of the surface which is covered by molecules. (We assume that $N_G/N \ll 1$.) The average energy of an evaporated atom is

$$\langle \epsilon \rangle = \Delta + kT. \quad (34)$$

The heat capacity is then

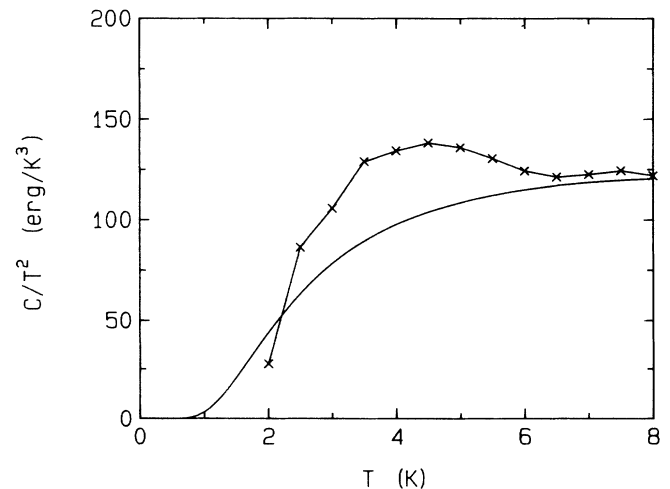


FIG. 11. Comparison of the heat capacity for 2D phonons with a low-frequency cutoff Eq. (32) (solid line) and experimental data (solid line with \times) for 0.51 mmol of H_2 in sample I.

$$C_{\text{evap}} = N_G k \left\{ \left[\left(\frac{\Delta}{kT} + 1 \right)^2 + 1 \right] - \frac{mkTa_m}{2\pi\hbar^2} e^{-\Delta/kT} \right\} / \left(1 - \frac{mkTa_m}{2\pi\hbar^2} e^{-\Delta/kT} \right). \quad (35)$$

In Fig. 12 we have plotted the data for sample I with 0.65 mmol of H_2 , together with C_{evap} given by Eq. (35). We have taken $\Delta = 22$ K (from Ni and Bruch²²) and $f = 0.5$. The evaporation heat capacity is substantially larger than the experimental data for temperatures greater than 5 K. In addition, C_{evap} is proportional to $(1-f)/f$ and thus decreases with increasing coverage f , whereas the experimental heat capacity is roughly proportional to f . It therefore appears that Eq. (35) must considerably overestimate C_{evap} . This is probably because the inhomogeneity of the substrate potential has been neglected. Thus, 22 K is the energy to take a molecule from an island to a point on the substrate *very near the edge* of the island. The energy to evaporate a molecule to most of the uncovered area of the substrate will be much larger. The result (35) overestimates C_{evap} by a factor²⁶ which is of order of $kT/\delta U$, where δU is the range of variation of the substrate potential. This factor is sufficient to make C_{evap} small compared to the experimental heat capacity.

E. Heat capacity above monolayer coverage

According to the calculations of Ni and Bruch²² the coverage n_m corresponding to an uncompressed monolayer is $11.6 \mu\text{mol m}^{-2}$. One can see from Fig. 9 that this corresponds approximately to the coverage at which the α , β , and γ phases meet at low temperatures. At higher temperature the coverage n_m thus lies in the α phase. This observation casts further doubt on the theory that the heat capacity in the α phase arises from 2D phonons. One would expect that for coverages above n_m the monolayer would be compressed, the sound velocity would increase, and the heat capacity would drop rapidly.

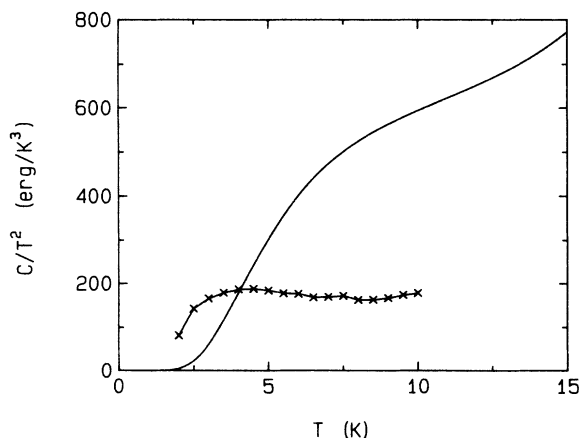


FIG. 12. Contribution to the heat capacity due to 2D evaporation from islands as given by Eq. (35) (solid line) together with experimental data (solid line with \times) for 0.65 mmol of H_2 in sample I. The evaporation energy is taken to be 22 K and the surface coverage f is $\frac{1}{2}$.

Using the calculations of Ni and Bruch²² we find that when the coverage is increased from the uncompressed monolayer up to $14 \mu\text{mol m}^{-2}$ the phonon heat capacity should drop by about a factor of 4. There is no sign of any such effect in the data, and in large pore Vycor in the higher part of the temperature range the heat capacity continues to increase with increasing coverage up to coverages close to $30 \mu\text{mol m}^{-2}$. Thus, the α phase includes coverages which range from a submonolayer to a compressed monolayer and on into the range beyond the limit of monolayer compression where some H_2 must go into a second layer. Because of the inhomogeneity of the substrate the transitions between the states will be smooth. Thus, before the monolayer is complete there will be regions in which, because the substrate potential is stronger, the monolayer is appreciably compressed. Similarly, the monolayer compression in the areas of weaker substrate potential will continue to increase while elsewhere molecules are being added to the second layer. Nevertheless, it seems hard to believe that the 2D phonon heat capacity can continue to increase up to $30 \mu\text{mol m}^{-2}$, since it appears to require unreasonably small sound velocities at high coverages.

Comparison can be made to the recent experiments of Ma *et al.*²⁷ of the heat capacity of H_2 adsorbed on a MgO substrate. For monolayers (which exhibited no freezing transition) and for approximately 1.5 monolayers (manifesting a freezing transition at ≈ 7.2 K) they found heat capacities in the 5 to 7 K range very similar in magnitude and temperature dependence as we observed with Vycor as the substrate. Presumably these heat capacities on very different substrates have a common explanation.

F. Freezing transitions

In samples I–III no freezing transitions were observed. In IV–VII two transitions were seen at temperatures T_{f1} and T_{f2} . It is natural to associate these transitions with the two peaks in the distribution of pore sizes, and further to assume that the lower freezing temperature T_{f1} is associated with the material in the smaller pores. It is believed²⁸ that due to silica dissolution during the leaching process in the production of Vycor glass, the larger set of pores (which we associate with the transition at T_{f2}) are situated near the surface of the Vycor. One can understand several features of the freezing transitions on the basis of this model. For low coverages the H_2 is in the form of a film throughout the sample. At a certain critical filling, capillary condensation begins to take place in the small pores. The freezing transition at T_{f1} then appears. As more material is added, the size of the peak at T_{f1} increases. Next, capillary condensation occurs in the larger pores, and the freezing transition at T_{f2} appears. Finally, when the Vycor is completely filled some H_2 remains outside the sample giving a sharp freezing transition at T_3 .

Freezing at a lower temperature in a smaller pore is expected on the basis of equilibrium thermodynamics. For a cylindrical pore of radius r the liquid and solid phases have equal free energy when²⁹

$$\delta F_{LS} = \frac{2v_s(\alpha_{SW} - \alpha_{LW})}{r}, \quad (36)$$

where δF_{LS} is the free-energy difference per molecule between the liquid and the solid, v_s is the volume per atom in the solid, and α_{SW} and α_{LW} are the surface energies between the pore wall and the solid and liquid, respectively. We can write

$$\alpha_{SW} = \alpha_{LW} + \alpha_{LS}\cos\theta, \quad (37)$$

where the contact angle θ is the angle between the liquid-solid interface and the wall, as measured in the liquid. Since δF_{LS} increases as the temperature goes below T_3 , Eq. (36) makes a prediction for the rate at which the freezing temperature drops as the pore radius decreases.

Two aspects of the data cannot be explained by this "equilibrium" model with two pore sizes. The heat capacities of samples IV, VI, and VII were also measured on warming. It was found that all of the transitions showed hysteresis, i.e., the melting temperatures were higher than the corresponding freezing temperatures. Secondly, there was a coupling between the two transitions. Thus, as soon as enough material was added for the T_{f2} transition to be observable, the temperature T_{f1} jumped to a high value. Similarly, the presence of bulk H_2 outside the Vycor which froze at T_3 , raised T_{f2} . Both of these effects indicate that the freezing is not entirely governed by equilibrium considerations, and that nucleation plays a role. When only the small pores are filled, nucleation has to occur in these pores in order for this material to freeze. However, if more H_2 is added so that the large pores are also filled, the solid that forms in these pores at T_{f2} can nucleate freezing in the small pores. Thus, T_{f1} is higher in this case. Similarly, the presence of bulk solid H_2 outside of the Vycor nucleates the freezing of H_2 in the large pores and raises T_{f2} .

The freezing process is presumably complicated by two other factors. The first is the fact that there is a distribution of radii within the groups of pores that we classify as small and large. This explains why T_{f1} increases slightly with increasing filling even before the transition at T_{f2} appears. The point is that the first small pores to fill will be those on the small side of the distribution, and these should have the lowest freezing temperatures. The lowest T_{f1} we have observed is 8.5 K in sample V for a filling such that the freezing peak has only just appeared. The second effect that must be important in a more complete understanding is the contraction that takes place when the liquid is cooled and when freezing occurs. This must leave the H_2 in the interior pores under a large negative pressure.

The shape of the peak in the heat capacity is qualitatively consistent with the nucleation picture. In Fig. 13 we show the freezing transition at T_{f1} for sample V with a filling of 2.70 mmol. The peak is much steeper on the

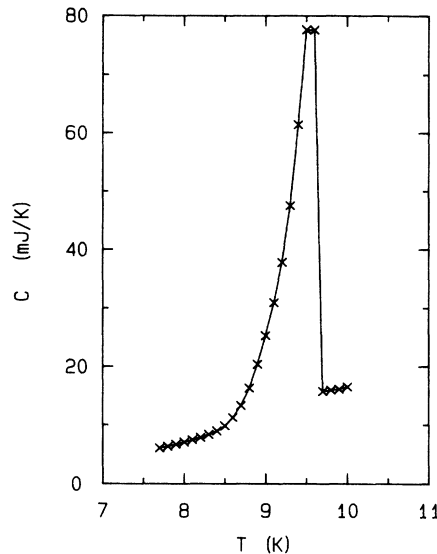


FIG. 13. A detailed plot of the freezing transition for sample V at T_{f1} . The sample contains 2.20 mmol of p - H_2 .

high-temperature side. We have constructed a simple model which qualitatively explains this behavior. We took a lattice of sites in which each site represents a pore filled with H_2 . We assumed that liquid in a pore can be represented by a nucleation site, a propagator site, or a stable site. A nucleation site is a pore of size such that solid H_2 will nucleate. A propagator site cannot nucleate solid but will become solid if an adjacent site is solid. A stable site is a pore which can neither nucleate or propagate. Thus, a propagator site is determined by the thermodynamic equilibrium condition. These sites are distributed randomly on the lattice. As the temperature decreases, the number N_p of propagator sites and the number N_N of nucleation sites will increase. We assume that $N_p \gg N_N$. At a critical value of N_p a percolation threshold is reached and although there is only a small density of nucleation sites, a larger number of sites suddenly convert from liquid to solid. This corresponds to the sudden rise in the heat capacity shown in Fig. 13 when the temperature has dropped to 9.6 K. At lower temperatures further increase of N_N and N_p gives a more gradual spread of solid sites, and a gradually decreasing heat capacity. By suitable choice of the distributions of temperatures at which sites become propagating or nucleating, one can obtain shapes for the heat capacity peak qualitatively similar to the experimental result.³⁰

For sample V we have calculated the integral of the heat capacity peak at $T_{f1} = 9.5$ K. This integral was found to vary linearly with the amount of H_2 in the sample over the range of fillings between the first appearance of the peak at T_{f1} and the appearance of the peak T_{f2} . If we assume that all of the added H_2 in this range goes into the small pores we can calculate the latent heat per mole at the T_{f1} transition. The result is $l_{LS} = 5.8$ K per molecule. The equilibrium thermodynamics model predicts [see Eq. (36)] that

$$I_{LS} = T\delta s_{LS} - \frac{2Tv_s}{r}(s_{SW} - s_{LW}), \quad (38)$$

where δs_{LS} is the entropy difference between liquid and solid per molecule, and s_{SW} and s_{LW} are the entropies per unit area of the interfaces between the Vycor wall and solid and liquid, respectively. Using the same method as described in Ref. 2, we calculate at T_{f1} that $T\delta s_{LS}$ is 6.6 K. The second term in Eq. (38) cannot be calculated accurately; however, a rough estimate³¹ suggests that its magnitude is less than 1 K. Thus, the agreement between Eq. (38) and the experimental result is reasonable.

G. Specific heat in the γ phase

In large-pore Vycor the existence of the freezing transition shows that the phase below T_{f1} (the γ phase) must be solid. The heat capacity in this phase *decreases* as more H_2 is added and varies as approximately T^3 [Fig. 7(b)]. As already noted, a phase whose heat capacity has similar characteristics exists in small-pore Vycor and thus it is natural to assume that this phase is also solid.

We have no explanation for the properties of the γ phase. The heat capacity of bulk solid H_2 is roughly proportional to T^3 in this temperature range³² but is only half the measured heat capacity for H_2 in small- or large-pore Vycor with the pores filled. In addition, the heat capacity in the γ phase is not proportional to the amount of material, in contrast to the behavior of bulk H_2 .

H. Torsional oscillator search for superfluidity

We have just argued, based upon the heat capacity measurements, that H_2 in the γ phase for small-pore Vycor is probably solid. Nevertheless, the fact that no freezing transition is observed does leave open some possibility that there is liquid H_2 in the Vycor. If there is liquid it may become superfluid and this transition can be detected through a measurement of the change in the moment of inertia of the Vycor and H_2 using the torsional oscillator technique. We have measured the changes in the oscillator frequency in the temperature range 1.5 to 6 K for three different H_2 fillings, and full Vycor down to 0.08 K (Fig. 14). These data show no sharp onset indicating superfluidity. The fractional frequency shift that occurred when enough H_2 was added to fill the cell was 65 ppm. From Fig. 9 we see that, even at low temperatures, the amount of H_2 involved in the γ phase is only 30% of the total. In addition, when superfluidity occurs, only a certain fraction³³ ($\approx 23\%$) of the H_2 should decouple from the motion of the Vycor. Thus, the expected frequency shift is only ≈ 4 ppm. The experimental results show that if there is a sharp transition at a temperature in the range down to 0.08 K, the magnitude of the frequency shift is less than 0.2 ppm.

The data do show two interesting features, however. When the H_2 is added to the cell, the temperature dependence of the oscillator frequency is larger than for the empty cell.³⁴ Thus, for example, the fractional frequency shift between 6 and 2 K is 0.88 ppm larger for full Vycor than for empty Vycor. This effect is much too big to be

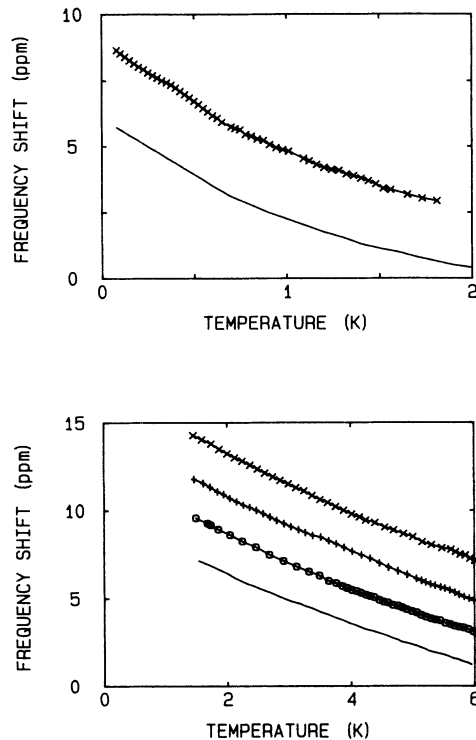


FIG. 14. Temperature dependence of the frequency of torsional oscillator containing various fillings of H_2 . Solid line denotes empty cell. (\times) 2.10 mmol (full), ($+$) 1.50 mmol, (\circ) 1 mmol. The data sets have been offset by different amounts to fit on the figure.

explained by the thermal expansion of H_2 , at least if the expansion is the same as that of bulk solid. The second effect observed was occasional jumps in the oscillator frequency of typical magnitude 0.1 to 1 ppm. These jumps *only* occurred when the H_2 filling was above a monolayer.

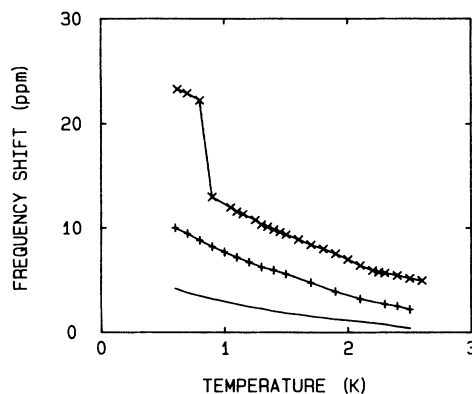


FIG. 15. Temperature dependence of the frequency of the torsional oscillator containing ^4He . Solid line denotes empty cell. (\times) 2.0 mmol (full), ($+$) 1 mmol (approximately a monolayer). The data sets have been offset by different amounts to fit on the figure.

We have no explanation for either of these effects.

One possible explanation of the absence of a freezing transition in small-pore Vycor is the idea that the pores are so small that essentially all of the molecules are adsorbed onto the walls. Another possibility is that tightly bound molecules on the walls block off the pores at so many places where the pores are unusually narrow that liquid cannot flow through the structure. To test whether this is the case, we studied ^4He in the same Vycor sample I. Results are shown in Fig. 15. A superfluid transition was found at 0.8 K. The magnitude of the frequency jump was 12 ppm, compared to the frequency shift of 150 ppm that occurred when the Vycor was filled with ^4He . As far as we know, this is the lowest superfluid transition temperature that has been found for ^4He completely filling a porous structure. The observation of the superfluid transition shows that, at least for ^4He , the pore structure is sufficiently open for liquid to exist and to flow.

V. SUMMARY

We have reported here extensive measurements of the heat capacity of $p\text{-H}_2$ in a series of porous Vycor glass samples. The principal experimental result is the observation of three distinct regions ("phases") in the filling-temperature (n - T) plane. These phases have similar

properties in all of the Vycor samples studied. In the α phase the heat capacity varies as T^2 and has a magnitude comparable to that expected from 2D phonons in a monolayer. However, as we have shown there are serious difficulties with this interpretation (see Secs. IV D and IV E). In the β phase (low coverage and low temperature) the heat capacity is essentially zero (i.e., too small to measure). The γ phase (high coverage and low temperature) appears to be solid. In large-pore Vycor various freezing transitions are observed and the temperatures of these transitions vary when the amount of H_2 in the pores is changed. The main features of these transitions can be understood in terms of the pore structure of the Vycor and nucleation processes. Finally, an investigation was made of the superfluid transitions of ^4He and H_2 in one of the small-pore Vycor samples. ^4He became superfluid at 0.8 K, but no transition was detected for H_2 down to 0.08 K.

ACKNOWLEDGMENTS

We thank Tom Elmer of Corning Glass for preparing the samples, L. W. Bruch for sending us the unpublished calculations of H_2 monolayer properties, and M. W. Cole and J. D. Reppy for helpful discussions. This work was supported in part by the National Science Foundation through Grant Nos. DMR-8719893 and DMR-8501858.

¹This is based on the observation that for a classical Lennard-Jones system the triple point is at $0.7 \epsilon_{\text{LJ}}/k_B$ (ϵ_{LJ} denotes Lennard-Jones energy).

²H. J. Maris, G. M. Seidel, and T. E. Huber, *J. Low Temp. Phys.* **51**, 471 (1983).

³J. L. Tell and H. J. Maris, *Phys. Rev. B* **28**, 5122 (1983).

⁴The results of Ref. 3 show that the melting temperature T_m (11.7 K) is appreciably higher than the freezing temperature. This hysteresis means that the suppression of the freezing temperature is not entirely governed by thermodynamics. However, the fact that T_m in Vycor is less than T_3 does mean that α_{LW} must be less than α_{SW} .

⁵T. H. Elmer, M. E. Nordberg, G. B. Carrier, and E. J. Korda, *J. Am. Ceram. Soc.* **53**, 171 (1970).

⁶This is the cleaning procedure suggested by Corning.

⁷We used the procedure by S. J. Gregg and K. S. W. Sing, *Absorption, Surface Area, and Porosity* (Academic, New York, 1967), Chaps. 3 and 4.

⁸W. F. Saam and M. W. Cole, *Phys. Rev. B* **11**, 1086 (1975).

⁹C. Pierce, *J. Chem. Phys.* **57**, 149 (1953).

¹⁰C. Orr and J. M. Dalla Valle, *Fine Particle Measurement* (Macmillan, London, 1959), p. 271.

¹¹S. J. Gregg and K. S. W. Sing, *Absorption, Surface Area, and Porosity*, Ref. 7, p. 165.

¹²R. Bachmann, F. J. DiSalvo, Jr., T. H. Geballe, R. L. Greene, R. E. Howard, C. N. King, H. C. Kirsch, K. N. Lee, R. E. Schwall, H. U. Thomas, and R. B. Zubeck, *Rev. Sci. Instrum.* **43**, 205 (1972).

¹³D. J. Bishop, J. E. Berthold, J. M. Parpia, and J. D. Reppy, *Phys. Rev. B* **24**, 5047 (1981).

¹⁴I. F. Silvera, *Rev. Mod. Phys.* **52**, 393 (1980).

¹⁵We have taken the average of this n for samples I and III in Fig. 9(a), and for V and VII in Fig. 9(b).

¹⁶R. H. Tait and J. D. Reppy, *Phys. Rev. B* **20**, 997 (1979).

¹⁷D. Finotello, A. Wong, K. A. Gillis, D. D. Awschalom, and M. H. W. Chan, *Jpn. J. Appl. Phys.* **26**, 283 (1987).

¹⁸D. Finotello, K. A. Gillis, A. Wong, and M. H. W. Chan, *Phys. Rev. Lett.* **61**, 1954 (1988).

¹⁹V. Ginzburg and A. A. Sobyenin, *Pis'ma Zh. Eksp. Teor. Fiz.* **15**, 343 (1972) [*Sov. Phys.—JETP Lett.* **15**, 242 (1972)].

²⁰This was reported in Ref. 3, and we have made some more measurements of this effect.

²¹L. A. Michels, W. de Graaf, and C. A. ten Seldam, *Physica* **26**, 393 (1960).

²²X.-Z. Ni and L. W. Bruch, *Phys. Rev. B* **33**, 4584 (1984).

²³The infrared absorption measurements of Huber and Huber show evidence of island formation at less than monolayer coverage. T. E. Huber and C. A. Huber, *Phys. Rev. Lett.* **59**, 1120 (1987).

²⁴Only values of B_2 for compressed monolayers were presented in Ref. 22. We thank Professor Bruch for communicating to us the result for an uncompressed monolayer [L. W. Bruch and J. M. Gottlieb (unpublished)].

²⁵Of course, one does not expect islands (other than very small ones) to be round.

²⁶This ratio is roughly the area adjacent to the islands, where the substrate potential is no more than kT above the potential at the island edge, divided by the total uncovered area.

²⁷J. Ma, D. L. Kingsbury, F. Liu, and O. E. Vilches, *Phys. Rev. Lett.* **61**, 2348 (1988).

²⁸T. Elmer (private communication).

²⁹We have neglected a correction in (36) which involves the differences in the molar volumes of the liquid and solid.

³⁰We hope to present more work with this model in a future publication.

³¹We have made this rough estimate using the model for the

temperature dependence of α_{LS} given in H. J. Maris, G. M. Seidel, and F. I. B. Williams, *Phys. Rev. B* **36**, 6799 (1987), and we have ignored the temperature dependence of the contact angle.

³²G. Ahlers, *J. Chem. Phys.* **41**, 86 (1964).

³³J. E. Berthold, D. J. Bishop, and J. D. Reppy, *Phys. Rev. Lett.*

39, 348 (1977).

³⁴For Vycor containing a low coverage of ^4He (i.e., insufficient for a superfluid transition to occur) a similar shift has been observed in experiments by J. Reppy (private communication).

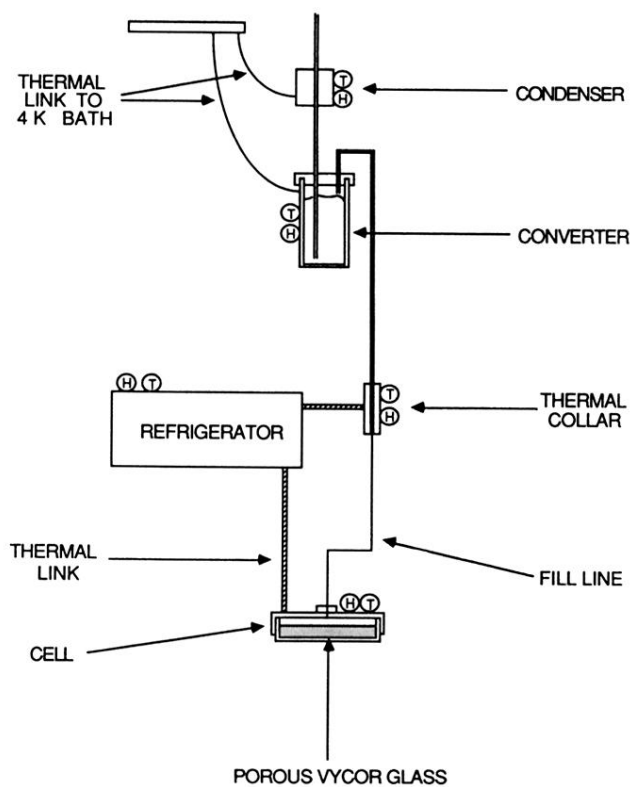


FIG. 2. Schematic diagram of the low-temperature heat capacity apparatus. The refrigerator was either a ^4He pot (1.5 K) or ^3He pot (0.5 K). H and T indicate heaters and thermometers, respectively.